

## Optimizing flow, strength, and durability in high-strength self-compacting and self-curing concrete utilizing lightweight aggregates

Syed Abdhaheer Kadhar<sup>1</sup> , Elangovan Gopal<sup>2</sup>, Vivek Sivakumar<sup>3</sup>, Naveen Arasu Anbarasu<sup>4</sup>

<sup>1</sup>University College of Engineering A.R. College of Engineering and Technology, Department of Civil Engineering, Kadayam, 627423, Tamil Nadu, India.

<sup>2</sup>University College of Engineering, Department of Civil Engineering, Pattukkottai, 614701, Tamil Nadu, India.

<sup>3</sup>GMR Institute of Technology, Department of Civil Engineering, Razam, 532127, Andhra Pradesh, India.

<sup>4</sup>CMS College of Engineering and Technology, Department of Civil Engineering, Coimbatore, 641032, Tamil Nadu, India.

e-mail: syedabdhaheerkadhar@gmail.com, abusvg@gmail.com, gelangoki@gmail.com, 1717vivek@gmail.com, naveenanbu07@gmail.com

---

### ABSTRACT

This comprehensive study undertaken to investigate the properties and performance of M60 grade self-compacting and self-curing concrete mix designs. The research involved an in-depth analysis of various concrete compositions labeled as M1 to M16, each with specific aggregate combinations and percentages. The primary focus was on assessing critical properties such as flow-ability, mechanical, durability and micro structural properties. The mix labeled as M6, featuring a balanced incorporation of fine aggregate alternatives (FAA) and natural coarse aggregates (NCA), exhibited noteworthy behavior in terms of the evaluated properties. This indicated the potential advantages of judiciously combining different types of aggregates to achieve desired concrete characteristics. The research underscored the critical role of aggregate selection and substitution in determining the overall durability, strength, and structural performance of M60 grade concrete. These findings contribute to an improved understanding of optimizing concrete mix designs for achieving enhanced mechanical properties, micro structural and long-term structural sustainability. The mix M12 is more superior compared to all the mix in the form of fresh concrete properties, mechanical properties and durability properties of concrete. This study's outcomes have implications for the construction industry, offering valuable insights into formulating concrete blends tailored for specific structural requirements and desired performance outcomes.

**Keywords:** Self-compacting and self-curing concrete; Light Weight Expanded; Clay aggregate and fly ash aggregate.

---

### 1. INTRODUCTION

Self-Compacting Concrete (SCC) is acclaimed for its exceptional flow and self-compacting attributes, eliminating external consolidation techniques. Integrating alternative aggregates like fly ash and expanded clay for conventional coarse aggregates has gained attention for sustainable construction. This blend capitalizes on SCC's benefits while enhancing eco-consciousness and cost-effectiveness. SCC's ability to flow effortlessly and fill complex forms transforms construction by eliminating manual vibration, expediting casting, and ensuring uniform concrete distribution [1–4]. Fly ash, a coal-fired power plant byproduct, enhances SCC's self-compacting properties and workability as a cementitious material. Including expanded clay aggregates replaces coarse aggregates, introducing qualities like reduced density, strength, and insulation. Combined with SCC, this yields a composite with lower weight, superior insulation, and enhanced structure. Self-curing concrete advances construction materials by streamlining curing and enhancing performance. Integrated innovative additives provide a practical solution to traditional curing, promoting resource efficiency and sustainability in construction [5–8].

Using Self-Compacting Mortar (SCM) materials—Meta Kaolin, Blast-furnace Slag, and fly ash—to replace cement in Self-Compacting Concrete (SCC). They found Metakaolin significantly improved compressive strength, making it a promising SCM. Both Metakaolin and Blast-furnace Slag also enhanced elasticity, except at 10% replacement of Blast-furnace Slag [9]. Using Granite Sawing Waste (GSW) and Polypropylene (PP) fibers in Fiber Reinforced Self-Compacting Concrete (FRSCC). GSW replaced cement at levels of 5%–20%,

and PP fibers at 0.05%–0.15% volume. Fly ash was also added. GSW and PP fibers improved compressive and splitting tensile strengths, along with fly ash, enhancing material properties [10]. Self-compacting concrete (SCC) with various additives and fibers to meet demands for efficient compaction around reinforcements in complex structures. Traditional methods face challenges in achieving thorough compaction, leading to voids. SCC, a self-flowing solution, eliminates external compaction. Their review emphasizes SCC's transformative role, enhancing compaction, quality, and efficiency in intricate construction [11]. Carbon fibers' effect on self-compacting concrete (SCC) toughness. Silica fume improved the cementitious mix. Carbon fibers (0–1.5%) strengthened and toughened the concrete. Their study unveiled synergistic performance enhancement from silica fume and carbon fibers in SCC [12].

Type F admixture and silica fume's impact on high early strength self-compacting concrete (SCC). ACEIVE 2018 conference presentation focused on their collaborative effects for expedited construction schedules. Through analysis, they highlighted potential for enhancing early-age strength, offering insights for robust SCC formulations in rapid construction projects [13]. The expansive self-compacting concrete using calcium sulfoaluminate. Diverse cementitious material dosages and curing methods were examined. Microstructural expansion improved compressibility and strength. Flexibility and compressive strength enhanced with expansion magnitude, while excessive dosages affected fresh air alteration [14]. Enhanced binder concrete durability using elevated cementitious materials and reduced water. Hydration acceleration caused permeability issues. Fly ash and rice husk waste facilitated 100% self-compacting concrete (SCC) hydration, promoting sustainability. Lightweight aggregates as internal curing improved strength and durability with W/b ratio < 0.36%. Cost-effective superabsorbent polymers (SAP) were highlighted as effective internal curing agents [15]. Self-compacting self-curing concrete advancements, emphasizing moisture absorption for hydration. Self-curing and self-compacting benefits offer efficient construction. Polyethylene glycol (PEG) optimizes curing, reducing water consumption. Best results involved 20% fly ash PEG with lower molecular weight, highlighting PEG's role in effective curing and water conservation [16]. Concrete grade, dosage, and curing agents' influence on normal and HSSC, self-curing concrete. Initial analysis assessed strength, followed by beam reinforcement. PEG 6000 emerged as more effective than PEG 4000 in achieving optimal strength, revealing curing agent importance for this innovative concrete type [17].

Fly ash's impact on self-compacting concrete (SCC) workability. Fly ash improved flowability, reducing excessive water needs while maintaining desired consistency. The study highlighted fly ash's potential as a sustainable addition to SCC, enhancing workability and promoting environmentally conscious construction [18]. Fly ash's impact on self-compacting concrete (SCC) mechanics. Fly ash improved compressive strength and durability through pozzolanic reactions and microstructure refinement. The study demonstrated fly ash's potential to enhance SCC's mechanical performance, promoting sustainable and high-performance construction practices [19]. Fly ash's ecological impact on self-compacting concrete (SCC). Analyzing carbon emissions associated with fly ash-infused SCC, they highlighted its potential to significantly reduce emissions compared CC due to fly ash's cement-reducing nature. Their findings advocate for fly ash in SCC to align with sustainable construction and emission reduction goals [20]. The rheological behavior of fly ash-infused SCC. They highlighted the importance of precise mix design and proportioning in achieving desired flow-ability and viscosity for effective self-placement and compaction. Through varied mix designs and fly ash levels, their research emphasized balanced approaches that optimize SCC with fly ash, enhancing its construction efficacy [21].

Synergies between fly ash and nano-silica in self-compacting concrete (SCC). Their study revealed combined potential to enhance strength and durability. By systematically investigating their interaction, the research showcased the promise of optimizing SCC's microstructure and mechanics through this partnership, offering a dynamic enhancement strategy for SCC [22]. The economic feasibility of fly ash incorporation in self-compacting concrete (SCC). Balancing initial costs with long-term benefits, the study revealed that despite a slight initial increase, fly ash-enhanced SCC's lasting advantages—improved durability and reduced maintenance—far outweighed the upfront difference. Their findings emphasized the strategic value of investing in fly ash-optimized SCC for long-term structural integrity and cost efficiency [23]. Expansive self-compacting concrete with calcium sulfo-aluminate ettringite. Variations in ettringite content affected characteristics and microstructure. Dosages, curing methods, and water-to-cementitious materials ratio influenced expansion and mechanics. Type K agents didn't impair workability but reduced W/C ratios with type K agents induced potentially problematic expansion. Elevated expansive agents caused expansion that compromised mechanical properties [24]. XRD and DTG analyses couldn't detect expansion. Anhydrous compounds induced expansion even after 28-day curing [25, 26]. Replaced cement with fly ash, blast furnace slag, and metakaolin, studying three expansive agent compositions. Agents improved pozzolanic activity, longevity, and mechanics, reducing autogenous shrinkage and enhancing chloride resistance. Shrinkage reduced due to refined porosity and desiccation, particularly with magnesia-based and liquid agents. The agents reduced V funnel time, enhancing slump flow. Sulpho-aluminate, polycarboxylate

ether, and magnesium agents improved elasticity and compressibility. Shrinkage tendencies were resolved by magnesium and polycarbonate agents, enhancing 28-day expansion [27].

Calcium-sulfoaluminates (CSA) and calcium oxide (CaO) expansion in ultra high performance concrete (UHPC). Factors like water-solid interactions, low W/b ratio, and compact structure impacted expansion. CaO with low water, a unique recessive nature, yielded expansive UHPC with strong structure and hydration. Study examined integrity, kinetics, strength, and volume traits [28]. CSA CaO curbed 24–28-hour auto shrinkage. Premature additives reduced efficacy, dryness increased shrinkage, and silica fume hindered kinetics. CaO with low water produced UHPC with minimal shrinkage [29]. Metakaolin and chemical admixtures for self-curing high-strength concrete. Metakaolin replaced cement (5%–15%), with optimal results at 5%. Poly-vinyl alcohol (PVA) and poly-acrylic acid (PAA) were added at various percentages. Best strengths were achieved with 0.04% PVA and 0.02% PAA. This approach enhances self-curing and strength in high-strength concrete [30]. Exploring internal curing in concrete using wood powder and polyethylene glycol 400 (PEG-400). M30 grade concrete underwent testing with varying wood powder (2%–8%) and PEG (0.5%–2.5%) ratios. Optimal outcomes were observed at 6% wood powder and 1.5% PEG for indoor conditions, and 6% wood powder and 2.5% PEG for outdoor conditions. This study underscores the potential of wood powder and PEG-400 in enhancing self-curing and concrete mechanical properties, thereby contributing to sustainable and durable concrete formulations [20]. Polyethylene Glycol (PEG) as a cement substitute for internal curing. They replaced cement with PEG-400 (0.5%–2%) in M30 grade concrete, evaluating axial, split tensile, and flexural strengths. Optimal results included 1% PEG-400 for axial and split tensile strengths, and 0.5% PEG-400 for flexural strength enhancement. This study highlights PEG-400's potential as an internal curing agent to enhance concrete properties and sustainability [31].

Self-Compacting Concrete (SCC) with alternative aggregates, like fly ash and expanded clay, optimizes sustainability and efficiency in construction. Metakaolin in Self-Compacting Concrete (SCC) boosts compressive strength, while Granite Sawing Waste and Polypropylene fibers enhance FRSCC properties. Metakaolin in high-strength concrete, replacing cement (5%–15%), achieves optimal results at 5%, enhanced by PVA and PAA. The main outcome of the research there is a lack of research with the SCC with self-curing concrete incorporating the recycled flyash concrete [32–35].

## 2. MATERIALS AND METHODS

This section deeply explores constituents like fly ash, expanded clay, and calotropis, alongside cement, fine and coarse aggregates, water, and additives, shaping concrete composition. Their properties influence concrete's behavior and performance [36]. The chapter highlights their roles in SCC and self-curing concrete. Fly ash enhances workability and durability through its pozzolanic properties. Expanded clay aggregates, low-density and porous, aid self-curing in SCC. Calotropis gigantea, a vegetative material, retains moisture for self-curing.

### 2.1. Cement

Cement, a vital concrete component, is meticulously chosen for this study. OPC grade 53 adhering to IS 12269 (1987) standard is used. OPC excels in binding constituents, providing strength and durability. OPC 53's high early strength and robustness make it optimal. Physically, it's dense, solid, and grey, with a specific gravity of 3.14, surface area of 2250 cm<sup>2</sup>/gm, and a particle size below 90 microns. A 3 mm volume expansion upon hydration and reactivity further define OPC 53's role in the study.

### 2.2. Fine aggregate

Fine aggregate selection significantly influences concrete properties. This study employed locally available river sand, ensuring cost-effectiveness and sustainability. Adhering to IS Grade Zone-II standards, the meticulously cleaned sand exhibited characteristics conducive to concrete quality. Its specific gravity, bulk density, water absorption, and fineness modulus were 2.75, 2.74 g/cc, 1.50%, and 1.52, respectively. The sand met specifications, passing a 4.75 mm sieve and being devoid of silt and clay. This careful selection establishes a foundation for producing concrete meeting performance criteria while upholding sustainability principles.

### 2.3. Coarse aggregate

The investigation delves into substituting traditional coarse aggregates with fly ash aggregates (as per IS 3812) and lightweight expanded clay aggregates. The process entails heating plastic clay in a rotating kiln to produce 12.5 mm expanded clay. Fly ash aggregates of the same size are generated with a 20:80 cement to fly ash ratio and 0.25 binder ratio. These innovative aggregates aim to enhance concrete attributes, exploring the prospects of heightened performance and durability. The mechanical traits of these materials are detailed in Table 1.

**Table 1:** Mechanical properties of coarse aggregates.

PROPERTIES	NCA	FAA	LECA
Size and Shape	12.5 mm & Angular	12.5 mm & Spherical	
Relative Density	2.65	1.34	1.45
WA (%)	1.74	20.5	32.5
CV (%)	17.54	18.49	12.8
Impact Strength (%)	14.70	16.69	14.795
Apparent Density (kg/m <sup>3</sup> )	1619	916	526
Moisture Content (%)	0.79	9.75	17.4
Fineness Modulus (%)	6.79	5.19	5.27

#### 2.4. Calotropis gigantia milk

A novel approach by incorporating *Calotropis gigantea* milk, a natural byproduct of the *Calotropis gigantea* plant found in Tamil Nadu, India. The milk contains polyethylene glycol latex, offering dual benefits of internal curing and enhanced water retention capacity in concrete. This resourceful utilization aligns with sustainable practices. This innovative technique holds potential for improved concrete performance and durability. *Calotropis gigantea* milk exhibits specific gravity of 1.1, solid content at  $3.5\% \pm 0.1\%$ , pH ranging from 7.19 to 8.21, and a characteristic white liquid appearance.

#### 2.5. Superplasticizers

The integral role of superplasticizers, particularly high-range water-reducing admixtures (HRWRAs), in High-Performance Concrete (HPC) formulation is paramount. Among them, Conplast SP430, classified as an effective plasticizer, significantly improves workability and performance. The specific gravity is 1.23. Applied at 2% by weight of cement, it modifies properties. Superplasticizers reduce water content while maintaining workability, often by up to 30%. Chosen here for practical mixtures with reduced water-to-binder (w/b) ratios, it enhances strength, durability, and performance. CONPLAST SP 430 adheres to ASTM C494 and IS: 9103–1998 standards, ensuring reliability. This dimension of versatility empowers high-performance mixtures, reshaping construction practices for more efficient and durable outcomes.

### 3. METHODOLOGY

The methodology encompasses the evaluation of flow-ability, mechanical, and durability properties of SCC and self-curing concrete. To assess flow-ability, tests such as slump flow, L-box, V-funnel, J-Ring, and U-box are conducted. Mechanical properties are measured through compressive, splitting tensile, and flexural strength tests (IS: 516, IS: 5816, IS: 516–1959). The durability analysis involves water absorption (IS: 2386) to evaluate porosity, rapid chloride permeability (ASTM C1202) to determine resistance to chloride penetration, acid resistance test and sorptivity testing. The micro analysis SEM is used to study the micro structural properties of concrete. This comprehensive testing approach facilitates a holistic understanding of the concrete's behavior, contributing to advancements in concrete technology and the development of sustainable construction materials. Table 2 shows the mix specifications. Based on the literature review and preliminary research the mix specifications have been decided.

#### 3.1. Fresh concrete test

The study employed the slump flow test to precisely assess Self-Compacting Concrete (SCC) filling capacity, flowability, and workability. A 500 mm diameter foundation plate, marked with a circle, served as the controlled testing platform. A specialized 300 mm high slump cone at the center of the plate housed the SCC mixture. Approximately six liters of SCC were gently poured into the cone, mimicking real-world scenarios. The stopwatch-recorded time for the SCC to complete a 500 mm diameter circle provided insights into its flowability and self-leveling capabilities.

#### 3.2. Mechanical properties of concrete

The compressive strength test gauges concrete's load-bearing capacity by applying controlled axial loads to specimens. Prepared cylinders or cubes undergo meticulous curing before being vertically positioned in a compressive testing apparatus. The applied load induces compressive stress, leading to deformations measured

**Table 2:** Mix specifications.

SI. NO.	MIX DESIGNATION	DESCRIPTION
1	M1	Conventional Concrete
2	M2	10% of Flyash Aggregate + 90% Natural Coarse Aggregate + 4% Calcotropis Gigantea + 2% Superplasticizer
3	M3	20% of Flyash Aggregate + 80% Natural Coarse Aggregate + 4% Calcotropis Gigantea + 2% Superplasticizer
4	M4	30% of Flyash Aggregate + 70% Natural Coarse Aggregate + 4% Calcotropis Gigantea + 2% Superplasticizer
5	M5	40% of Flyash Aggregate + 60% Natural Coarse Aggregate + 4% Calcotropis Gigantea + 2% Superplasticizer
6	M6	50% of Flyash Aggregate + 50% Natural Coarse Aggregate + 4% Calcotropis Gigantea + 2% Superplasticizer
7	M7	10% of Lightweight Expanded Clay Aggregates + 90% Natural Coarse Aggregate + 4% Calcotropis Gigantea + 2% Superplasticizer
8	M8	20% of Lightweight Expanded Clay Aggregates + 80% Natural Coarse Aggregate + 4% Calcotropis Gigantea + 2% Superplasticizer
9	M9	30% of Lightweight Expanded Clay Aggregates + 70% Natural Coarse Aggregate + 4% Calcotropis Gigantea + 2% Superplasticizer
10	M10	40% of Lightweight Expanded Clay Aggregates + 60% Natural Coarse Aggregate + 4% Calcotropis Gigantea + 2% Superplasticizer
11	M11	50% of Lightweight Expanded Clay Aggregates + 50% Natural Coarse Aggregate + 2% Calcotropis Gigantea + 2% Superplasticizer
12	M12	10% of Flyash Aggregate + 10% of Lightweight Expanded Clay Aggregates + 80% Natural Coarse Aggregate + 4% Calcotropis Gigantea + 2% Superplasticizer
13	M13	20% of Flyash Aggregate + 20% of Lightweight Expanded Clay Aggregates + 60% Natural Coarse Aggregate + 4% Calcotropis Gigantea + 2% Superplasticizer
14	M14	30% of Flyash Aggregate + 30% of Lightweight Expanded Clay Aggregates + 40% Natural Coarse Aggregate + 4% Calcotropis Gigantea + 2% Superplasticizer
15	M15	40% of Flyash Aggregate + 40% of Lightweight Expanded Clay Aggregates + 20% Natural Coarse Aggregate + 4% Calcotropis Gigantea + 2% Superplasticizer
16	M16	50% of Flyash Aggregate + 50% of Lightweight Expanded Clay Aggregates + 0% Natural Coarse Aggregate + 4% Calcotropis Gigantea + 2% Superplasticizer

by strain gauges or sensors. The correlation between load and deformation yields the ultimate compressive strength, vital for assessing compressive, splitting tensile and flexural strength test.

### 3.3. Durability properties of concrete

To ensure the durability of concrete, meticulous steps are taken from material selection to regular maintenance. High-quality ingredients, optimal mix design, and incorporation of admixtures like air-entraining agents contribute to enhanced resistance against environmental factors. Rigorous testing saturated water absorption, acid resistance, sorptivity, porosity and rapid chloride penetration test ensures the concrete's robustness. Additionally, measures such as corrosion protection for reinforcement and regular inspections contribute to long-lasting, structurally sound concrete, safeguarding against deterioration in diverse environmental conditions.

## 4. RESULTS AND DISCUSSION

### 4.1. Flow-ability test

#### 4.1.1. Slump cone test

The study conducted an in-depth analysis of sixteen distinct concrete mixtures, labeled M1 to M16, to examine the effect of varying aggregate proportions and chemical admixtures on slump flow. The combinations included conventional aggregates, fly ash aggregates (FAA), lightweight expanded clay aggregates (LWECA), calotropis gigantea (CG), and superplasticizer (SP). The results revealed a notable correlation between the composition of the mixtures and their workability. As the proportions of FAA, LWECA, and combined additives increased, the slump flow also improved, indicating enhanced workability and flow characteristics. These findings underline the potential for tailoring concrete mix designs to optimize workability and performance for specific construction requirements. Notably, the proportion of LWECA within the mix exerts a significant influence on deformability and stability. As the content of LWECA increases, there is a trend towards improved deformability, indicated by the incrementally larger slump value. Mix designs like M10, M11, and M16, characterized by higher LWECA content, exhibit noticeably larger slump value in comparison to conventional concrete and mixes dominated by FAA content. Figure 1 shows the slump cone test results of M60 grade concrete [37].

#### 4.1.2. L box test

The study involved an extensive investigation into sixteen concrete mixtures labeled M1 to M16, aiming to assess their workability using the L-box test. These mixtures encompassed various combinations of aggregates, additives, and superplasticizer (SP). The results indicated that as the proportions of fly ash aggregates (FAA),

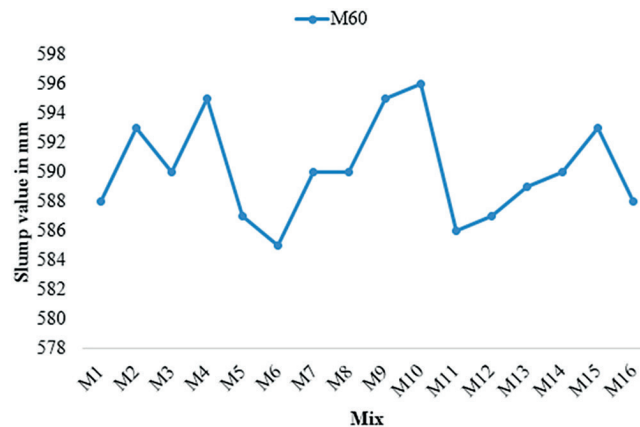


Figure 1: Slump cone test results.

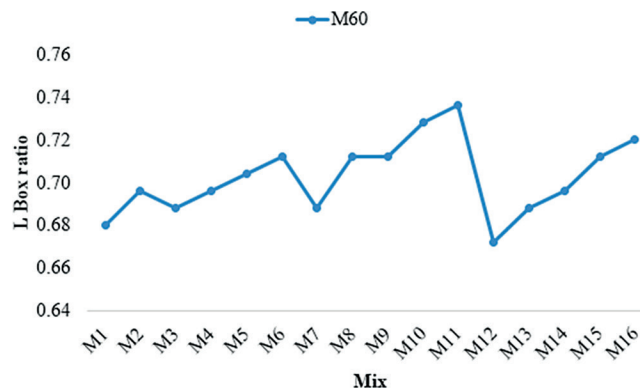


Figure 2: L box test results.

lightweight expanded clay aggregates (LWECA), calcotropis gigantea (CG), and SP were altered, the workability of the concrete mixtures exhibited variations [38]. The L-box test outcomes demonstrated an intricate relationship between the composition of the mixtures and their ability to flow and spread, highlighting the role of aggregates and additives in influencing concrete workability. These findings contribute to a better understanding of optimizing concrete mix designs for desired workability characteristics in construction applications. The influence of LWECA content is further evident in the incremental increase in passing ability as the LWECA content is raised, as seen in the progression from M7 to M11. Figure 2 shows the test results of L box test.

#### 4.1.3. V-Funnel test

The workability characteristics of various concrete mixtures labeled M1 to M16, as determined by the V-funnel test. The results highlight the substantial impact of altering aggregate proportions, additives, and superplasticizer (SP) content on the flow behavior of the concrete. Notably, the workability, represented by the V-funnel test duration, exhibited variations based on these factors. The V-funnel test outcomes provide a comprehensive overview of how different combinations of aggregates and additives influence the ease of concrete flow and its ability to pass through constrictions, reflecting the intricate interplay between mixture components and their effect on concrete workability [39]. These findings contribute to a more informed approach to designing concrete mixtures that align with desired workability requirements for construction applications. Mix designs such as M10, M11, M12, and M13, characterized by higher LWECA content, distinctly exhibit reduced V-Funnel test times relative to conventional concrete and mixes dominated by FAA content. Figure 3 shows the result of v-funnel test.

#### 4.1.4. J-Ring

The stability and resistance to segregation during casting of concrete mixes with the labels M1 to M16 may be learned a lot from the examination of J-Ring test results. J-Ring values can vary depending on the aggregate quantities and additives used, including superplasticizer (SP). The measures represent the cohesiveness of the concrete, which keeps the coarse aggregate from separating under self-compacting and self-curing circumstances. These results underline the significance of aggregate combinations and additives in maintaining uniformity and stability during placement, enhancing casting performance, and improving the general quality of concrete. Notably, the proportion of LWECA within the mix emerges as a significant influencer of passing ability and stability. A trend becomes apparent as the LWECA content escalates, correlating with improved passing ability. This trend is evident from slightly elevated J-Ring measurements observed in mix designs such as M10, M11, M12, and M13. These formulations, characterized by heightened LWECA content, manifest relatively larger J-Ring measurements compared to conventional concrete and mixes enriched with FAA content. For a graphic representation of the J-Ring test findings, see Figure 4.

#### 4.1.5. U-Box

The U-Box test results for concrete mixtures designated from M1 to M16 offer valuable insights into the stability and deformability of these mixtures. The measured U-Box values reflect the responsiveness of the concrete to flow and deformation under the influence of varying aggregate combinations and additives, including superplasticizer (SP). The obtained measurements illustrate the ability of each mixture to maintain its form and structure

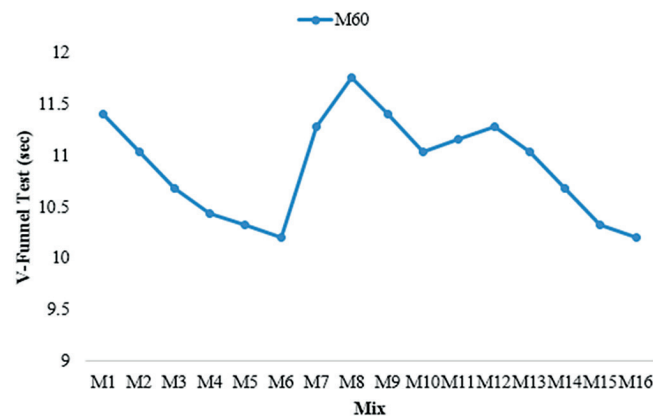


Figure 3: V-Funnel test results.

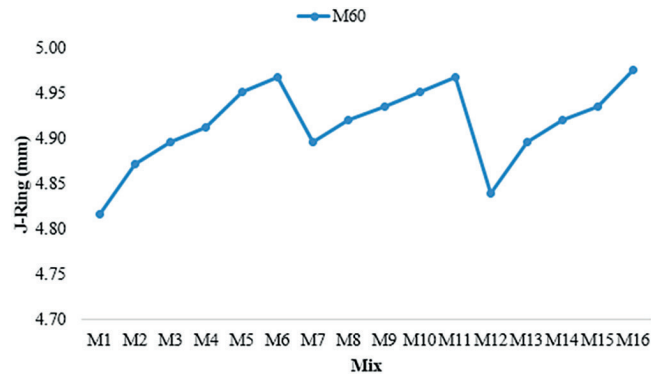


Figure 4: J-ring Test results.



Figure 5: U-Box test results.

while flowing into the U-Box apparatus, which simulates a practical casting scenario. These findings underscore the role of specific aggregate combinations and additives in determining the concrete’s flow characteristics and stability during placement, thus contributing to improve casting performance and enhanced overall concrete quality. Notably, the proportion of LWECA within the mix exerts a significant influence on deformability and stability. As the content of LWECA increases, there is a trend towards improved deformability, indicated by the incrementally larger U-Box measurements. Mix designs like M10, M11, and M16, characterized by higher LWECA content, exhibit noticeably larger U-Box measurements in comparison to conventional concrete and mixes dominated by FAA content. Figure 5 visually presents the outcomes of the U-Box tests, further elucidating the impact of the studied parameters on concrete behavior.

## 4.2. Mechanical properties of concrete

### 4.2.1. Compression strength test

The compressive strength test outcomes offer insight into the mechanical performance of distinct concrete mixes, particularly for M60 grade, across varying curing periods. Mixes with higher lightweight expanded clay aggregate (LWECA) content, like M7, M8, and M12, exhibit superior strengths at 7, 14, and 28 days. In summary, the results underscore LWECA’s positive influence on strength in self-consolidating concrete, though comprehensive evaluation remains pivotal for practical application. Figure 6 visually presents the outcomes of the compressive strength tests, further elucidating the impact of the studied parameters on concrete behavior.

### 4.2.2. Split tensile strength

The split tensile strength test outcomes unveil the mechanical characteristics of distinct concrete mixes for M60 grade over different curing periods. Mixes with elevated lightweight expanded clay aggregate (LWECA) content, like M7, M8, and M12, exhibit notable improvements in split tensile strengths at 7, 14, and 28 days. Yet, it’s vital to recognize that factors such as durability and workability significantly influence mix selection. In summary,

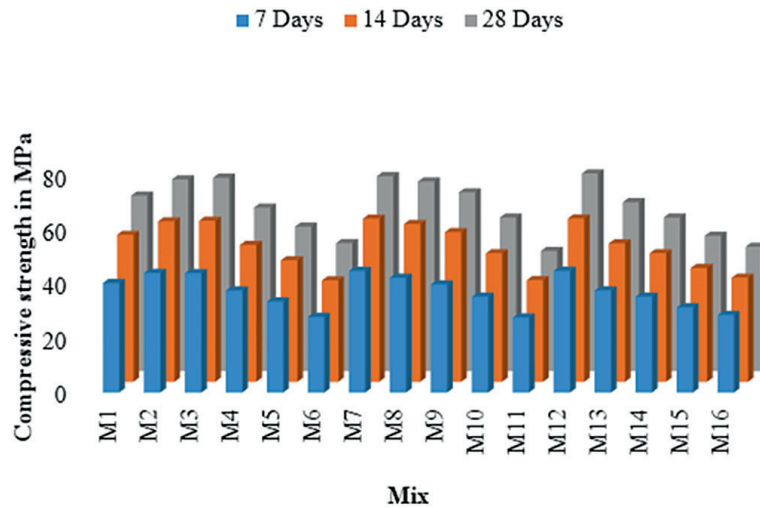


Figure 6: Compression strength test results.

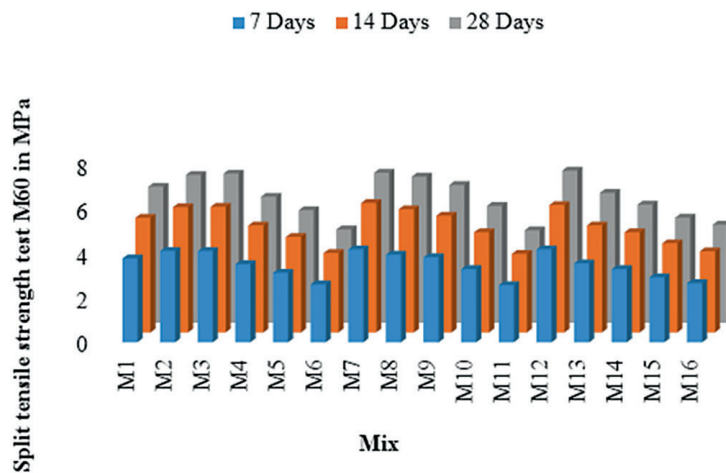


Figure 7: Split tensile strength results.

the results underscore LWECA’s constructive impact on split tensile strength within self-consolidating concrete, stressing the need for a comprehensive assessment for practical applications. Figure 7 visually represent the nuanced variations in split tensile test results.

#### 4.2.3. Flexural strength test

The flexural strength test outcomes elucidate the structural behavior of diverse concrete mixtures for M60 grade, spanning multiple curing periods. Mix designs enriched with higher lightweight expanded clay aggregate (LWECA) ratios, like M7, M8, and M12, exhibit notable improvements in flexural strengths at 7, 14, and 28 days. Nevertheless, it’s vital to recognize that mix selection is also influenced by aspects such as durability and workability. In essence, the findings underscore LWECA’s positive influence on flexural strength within self-consolidating concrete, emphasizing the necessity for a comprehensive assessment in practical applications. Figure 8 visually depict the nuanced variations in flexural strength test results.

#### 4.3. Durability test

##### 4.3.1. Saturated water absorption

The data highlights varying water absorption percentages across different mix designs and curing durations. Conventional concrete (M1) showed a 2.31% water absorption at 28 days, decreasing to 1.99% at 90 days. Generally, increased proportions of fine aggregate alternatives (FAA) or lightweight expanded clay aggregate

(LWECA) led to reduced water absorption. Mix M6, comprising 50% FAA and 50% natural coarse aggregate (NCA), exhibited a 2.51% water absorption at 28 days, decreasing to 2.17% at 90 days. The introduction of LWECA also influenced water absorption. For example, mix M11, with 50% LWECA and 50% NCA, demonstrated a 2.53% water absorption at 28 days, decreasing to 2.18% at 90 days. The data underscores the significant role of aggregate types and proportions in water absorption characteristics, contributing valuable insights for mix design optimization tailored to specific project requirements. Figure 9 visually depicts the nuanced variations in saturated water absorption test results.

### 4.3.2. Porosity

The results exhibit variations in porosity among the mix designs and curing durations. Conventional concrete (M1) displayed a porosity of 3.91% at 28 days, which decreased to 3.01% at 90 days. The introduction of fine aggregate alternatives (FAA) or lightweight expanded clay aggregate (LWECA) generally led to a reduction in porosity. For instance, mix M6, consisting of 50% FAA and 50% natural coarse aggregate (NCA), displayed a porosity of 4.25% at 28 days, decreasing to 3.46% at 90 days. Furthermore, the incorporation of LWECA influenced porosity. Mix M11, composed of 50% LWECA and 50% NCA, exhibited a porosity of 4.31% at 28 days, which decreased to 3.49% at 90 days. The data underscores the substantial impact of aggregate types and proportions on porosity characteristics, offering insights for refining mix designs according to specific project requirements. Figure 10 visually depicts the nuanced variations in porosity test results.

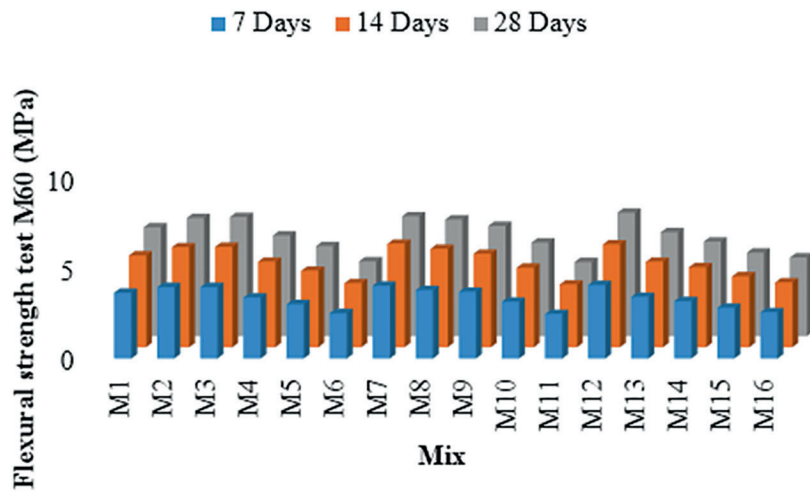


Figure 8: Flexural strength test results.

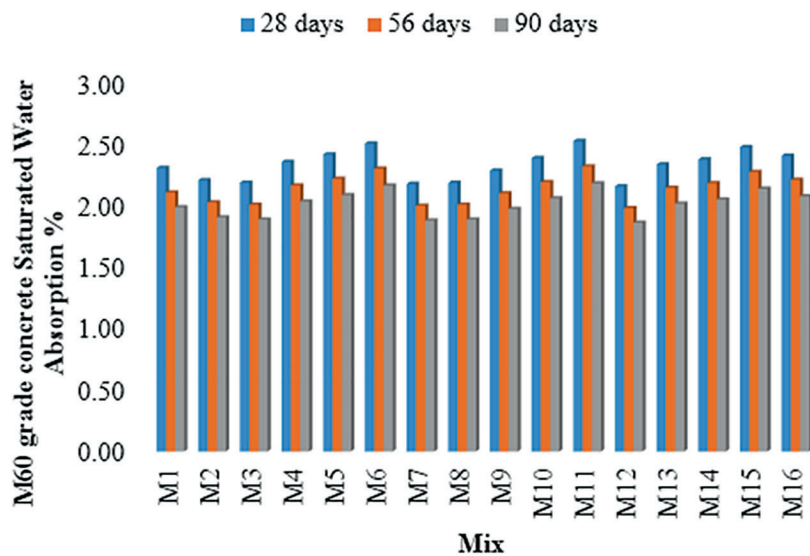


Figure 9: Saturated water absorption.

### 4.3.3. Acid resistance

The findings reveal fluctuations in weight loss percentages across mix designs and curing durations. Conventional concrete (M1) showed a weight loss of 3.03% at 28 days, declining to 2.32% at 90 days. Introducing fine aggregate alternatives (FAA) or lightweight expanded clay aggregate (LWECA) generally led to marginal variations in weight loss. For example, mix M6, composed of 50% FAA and 50% natural coarse aggregate (NCA), displayed a weight loss of 3.30% at 28 days, decreasing to 2.66% at 90 days. The data underscores how aggregate types and proportions influence weight loss characteristics. Figure 11 visually depict the nuanced variations in % of loss of weight.

### 4.3.4. Sorptivity test

The findings reveal variations in sorptivity percentages across different mix designs and curing durations. Conventional concrete (M1) exhibited a sorptivity of 0.096 at 28 days, which decreased to 0.067 at 90 days. Incorporating fine aggregate alternatives (FAA) or lightweight expanded clay aggregate (LWECA) generally led to minor fluctuations in sorptivity. For instance, mix M6, composed of 50% FAA and 50% natural coarse aggregate (NCA), demonstrated a sorptivity of 0.112 at 28 days, increasing to 0.092 at 90 days. The data underscores the influence of aggregate types and proportions on sorptivity characteristics, providing insights for optimized mix design considerations. Figure 12 visually depict the nuanced variations in sorptivity test results.

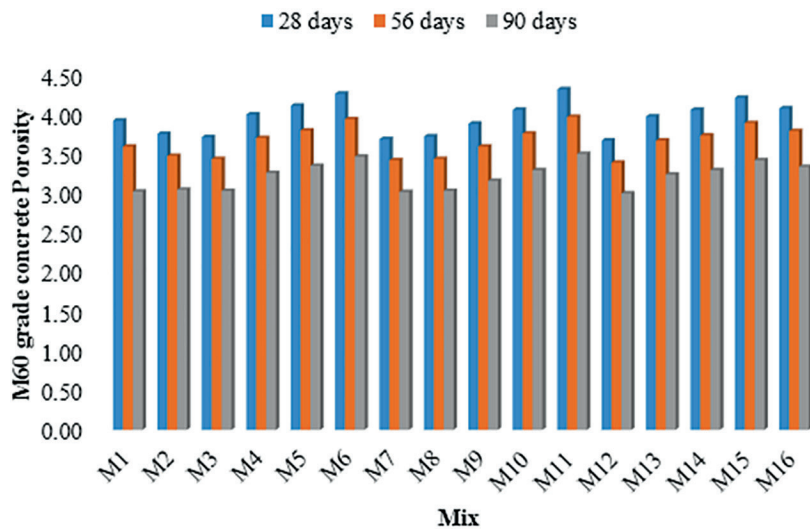


Figure 10: Potosity properties of the concrete.

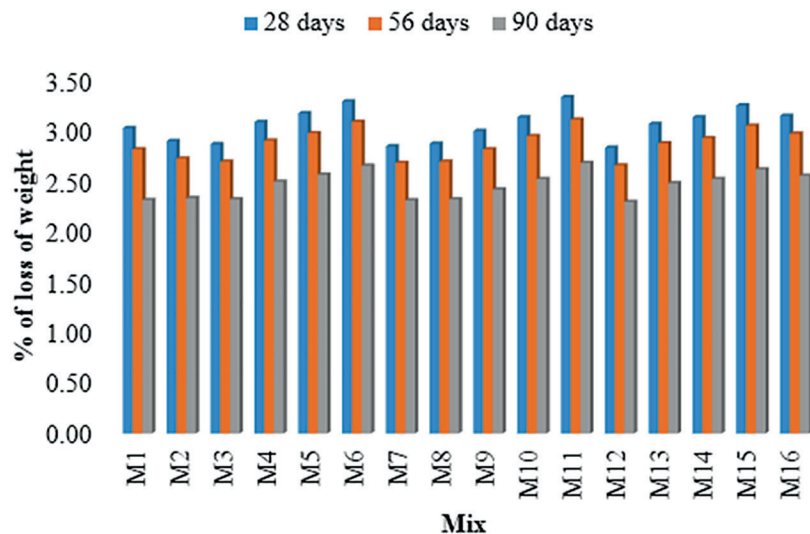


Figure 11: Percentnage loss of weight.

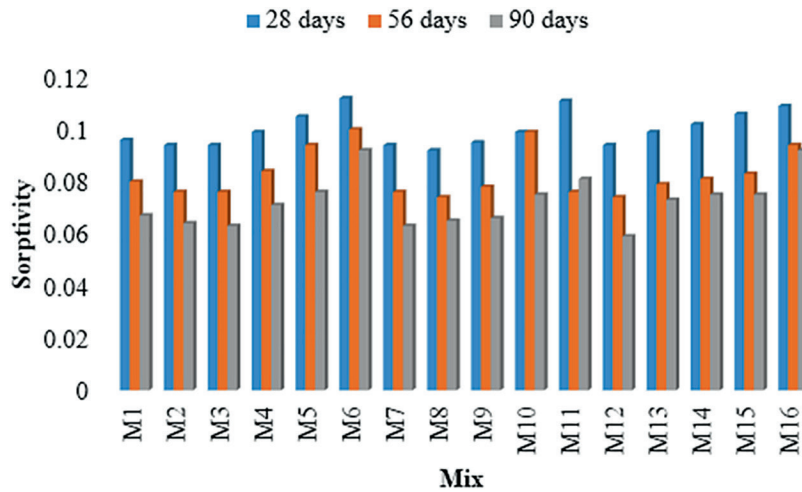


Figure 12: Sorptivity test of concrete.

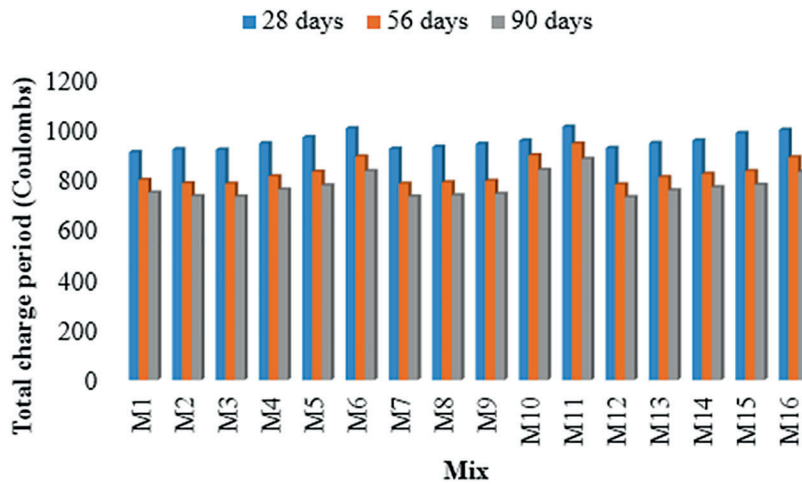


Figure 13: Rapid Chloride Penetration Test.

#### 4.3.5. Rapid chloride penetration test

The findings illustrate variations in total charge periods attributed to distinct mix compositions. Standard concrete (M1) exhibited total charge periods of 910 Coulombs at 28 days, diminishing to 748 Coulombs at 90 days. Formulations involving substitutions like fine aggregate alternatives (FAA) or lightweight expanded clay aggregate (LWECA) displayed slight fluctuations in total charge periods. Remarkably, mixture M6, comprising 50% FAA and 50% natural coarse aggregate (NCA), presented a total charge period of 1005 Coulombs at 28 days, which reduced to 834 Coulombs at 90 days. The outcomes underscore the influence of aggregate types and ratios on the overall charge characteristics of concrete blends. Figure 13 visually depicts the nuanced variations in RCPT test results.

#### 4.4. Microstructure analysis

##### 4.4.1. SEM

The Scanning Electron Microscope (SEM) has proven to be an invaluable tool for the detailed analysis of concrete structures, as evidenced by the compelling images presented in Figures 14 and 15. These images shed light on the intricate microstructural differences between standard concrete, M12 mix, and SCC mixes. In the case of standard concrete, Figure 14 reveals a somewhat disorganized particle distribution, accompanied by a higher prevalence of pores. These pores exhibit a relatively larger diameter, spanning from 3 to 4.25  $\mu\text{m}$ . This observation suggests that standard concrete may be more susceptible to structural weaknesses due to its porous nature.

On the other hand, Figure 15 showcases SEM images of the M12 mix, where a notable improvement in the bond between the cement matrix and aggregates is evident. However, not without its imperfections, the M12 mix still exhibits the presence of pores and cracks within the cement matrix. Notably, these pores possess a smaller diameter, measuring between 0.95 and 2.5  $\mu\text{m}$ , suggesting that the M12 mix may offer enhanced structural integrity compared to standard concrete [40]. These findings underscore the critical role of SEM analysis in elucidating the intricate characteristics of concrete mixes, aiding in their optimization and overall improvement.

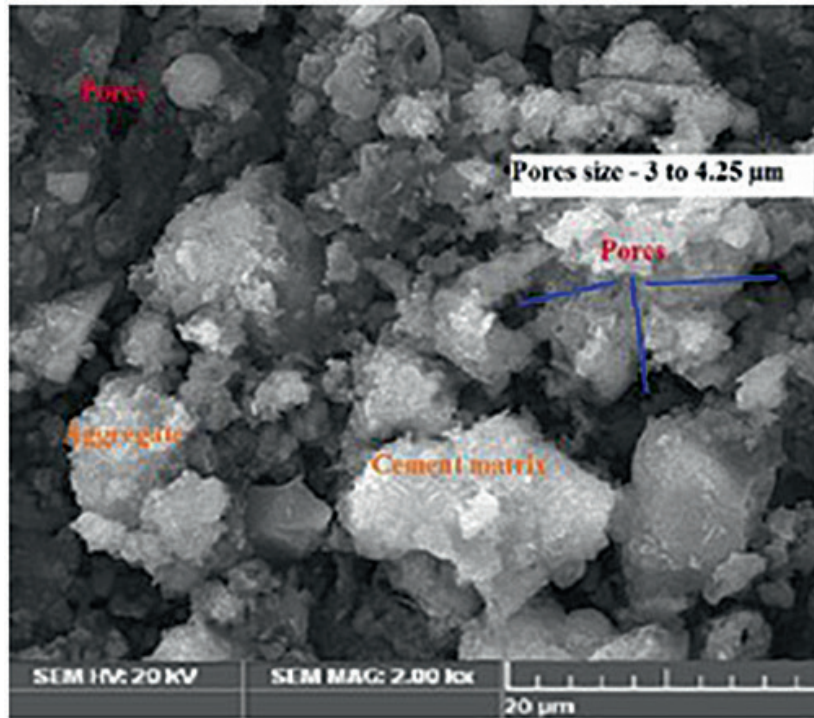


Figure 14: SEM image of standard concrete.

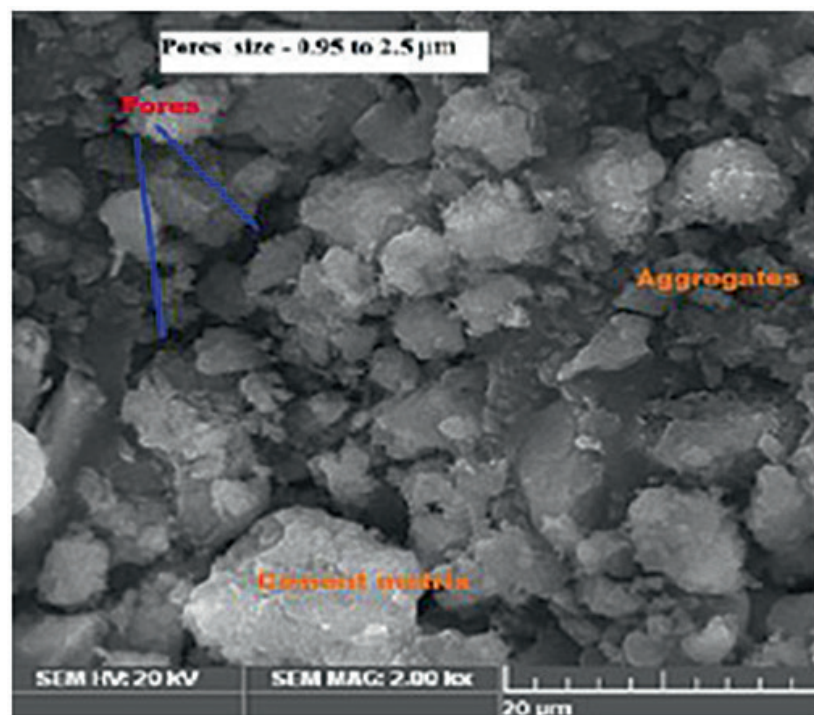


Figure 15: SEM image of M12 mix.

## 5. CONCLUSION

The conclusions drawn from this study are explained below:

The introduction of *Calotropis gigantea* milk into SCC has improved the self-curing properties of the concrete. Mix designs like M10, M11, and M16, characterized by higher LWECA content, exhibit noticeably larger flow-ability in comparison to conventional concrete and mixes dominated by FAA content. Mix designs enriched with higher lightweight expanded clay aggregate (LWECA) ratios, like M7, M8, and M12, exhibit notable improvements in mechanical properties like compressive strength, split tensile strength and flexural strengths at 7, 14, and 28 days. Conventional concrete (M1) showed a 2.31% water absorption at 28 days, decreasing to 1.99% at 90 days. Mix M6, comprising 50% FAA and 50% natural coarse aggregate (NCA), exhibited a 2.51% water absorption at 28 days, decreasing to 2.17% at 90 days. The introduction of LWECA also influenced water absorption. The results exhibit variations in porosity among the mix designs and curing durations. Conventional concrete (M1) displayed a porosity of 3.91% at 28 days, which decreased to 3.01% at 90 days. For instance, mix M6, consisting of 50% FAA and 50% natural coarse aggregate (NCA), displayed a porosity of 4.25% at 28 days, decreasing to 3.46% at 90 days. The findings reveal fluctuations in weight loss percentages across mix designs and curing durations. Conventional concrete (M1) showed a weight loss of 3.03% at 28 days, declining to 2.32% at 90 days. The findings reveal variations in sorptivity percentages across different mix designs and curing durations. Conventional concrete (M1) exhibited a sorptivity of 0.096 at 28 days, which decreased to 0.067 at 90 days. The findings reveal variations in sorptivity percentages across different mix designs and curing durations. Conventional concrete (M1) exhibited a sorptivity of 0.096 at 28 days, which decreased to 0.067 at 90 days. The findings illustrate variations in total charge periods attributed to distinct mix compositions. Standard concrete (M1) exhibited total charge periods of 910 Coulombs at 28 days, diminishing to 748 Coulombs at 90 days. Microstructural differences between standard concrete and M12 mix. Standard concrete exhibits larger pores (3–4.25  $\mu\text{m}$ ), potentially impacting its structural integrity. In contrast, M12 mix displays improved cement-aggregate bonding but still has smaller pores (0.95–2.5  $\mu\text{m}$ ), suggesting enhanced structural integrity. SEM analysis is vital for optimizing concrete mixes. The mix M12 (10% of Flyash Aggregate + 10% of Lightweight Expanded Clay Aggregates + 80% Natural Coarse Aggregate + 4% *Calotropis Gigantea* + 2% Superplasticizer) is more superior compared to all the mix in the form of fresh concrete properties, mechanical properties and durability properties of concrete.

## 6. BIBLIOGRAPHY

- [1] LIU, C., CUI, J., ZHANG, Z., *et al.*, “The role of TBM asymmetric tail-grouting on surface settlement in coarse-grained soils of urban area: Field tests and FEA modelling”, *Tunnelling and Underground Space Technology*, v. 111, pp. 103857, 2021. doi: <http://dx.doi.org/10.1016/j.tust.2021.103857>.
- [2] HE, H., E, S., WEN, T., *et al.*, “Employing novel N-doped graphene quantum dots to improve chloride binding of cement”, *Construction & Building Materials*, v. 401, pp. 132944, 2023. doi: <http://dx.doi.org/10.1016/j.conbuildmat.2023.132944>.
- [3] HE, H., SHI, J., YU, S., *et al.*, “Exploring green and efficient zero-dimensional carbon-based inhibitors for carbon steel: from performance to mechanism”, *Construction & Building Materials*, v. 411, pp. 134334, 2024. doi: <http://dx.doi.org/10.1016/j.conbuildmat.2023.134334>.
- [4] WANG, M., YANG, X., WANG, W., “Establishing a 3D aggregates database from X-ray CT scans of bulk concrete”, *Construction & Building Materials*, v. 315, pp. 125740, 2022. doi: <http://dx.doi.org/10.1016/j.conbuildmat.2021.125740>.
- [5] TANG, Y., WANG, Y., WU, D., *et al.*, “Exploring temperature-resilient recycled aggregate concrete with waste rubber: an experimental and multi-objective optimization analysis”, *Reviews on Advanced Materials Science*, v. 62, n. 1, pp. 20230347, 2023. doi: <http://dx.doi.org/10.1515/rams-2023-0347>.
- [6] ZHANG, J., ZHANG, C., “Using viscoelastic materials to mitigate earthquake-induced pounding between adjacent frames with unequal height considering soil-structure interactions”, *Soil Dynamics and Earthquake Engineering*, v. 172, pp. 107988, 2023. doi: <http://dx.doi.org/10.1016/j.soildyn.2023.107988>.
- [7] LIN, J., CHEN, G., PAN, H., *et al.*, “Analysis of stress-strain behavior in engineered geopolymer composites reinforced with hybrid PE-PP fibers: a focus on cracking characteristics”, *Composite Structures*, v. 323, pp. 117437, 2023. doi: <http://dx.doi.org/10.1016/j.compstruct.2023.117437>.
- [8] DADSETAN, S., BAI, J., “Mechanical and microstructural properties of self-compacting concrete blended with metakaolin, ground granulated blast-furnace slag and fly ash”, *Construction & Building Materials*, v. 146, pp. 658–667, 2017. doi: <http://dx.doi.org/10.1016/j.conbuildmat.2017.04.158>.

- [9] KARMEGAM, A., KALIDASS, A., “Reusing granite sawing waste in self-compacting concrete with polypropylene fiber at low-volume fractions”, *Structural Concrete*, v. 20, n. 2, pp. 766–773, 2019. doi: <http://dx.doi.org/10.1002/suco.201800155>.
- [10] ARULSIVANANTHAM, P., GOKULAN, R., “A review on self-compacting concrete”, *International Journal of Chemtech Research*, v. 10, pp. 62–68, 2018.
- [11] GUNEYISI, E., GESOGLU, M., FAHMI, M., *et al.*, “Mechanical and fracture properties of carbon fiber reinforced self-compacting concrete composites”, In: *10th International Conference on Composite Science and Technology*, Lisboa, Portugal, 2015.
- [12] PANG, B., ZHENG, H., JIN, Z., *et al.*, “Inner superhydrophobic materials based on waste fly ash: microstructural morphology of microetching effects”, *Composites. Part B, Engineering*, v. 268, pp. 111089, 2024. doi: <http://dx.doi.org/10.1016/j.compositesb.2023.111089>.
- [13] HUANG, H., HUANG, M., ZHANG, W., *et al.*, “Progressive collapse resistance of multistory RC frame strengthened with HPFL-BSP”, *Journal of Building Engineering*, v. 43, pp. 103123, 2021. doi: <http://dx.doi.org/10.1016/j.job.2021.103123>.
- [14] HUANG, H., GUO, M., ZHANG, W., *et al.*, “Numerical investigation on the bearing capacity of RC columns strengthened by HPFL-BSP under combined loadings”, *Journal of Building Engineering*, v. 39, pp. 102266, 2021. doi: <http://dx.doi.org/10.1016/j.job.2021.102266>.
- [15] GUO, M., HUANG, H., ZHANG, W., *et al.*, “Assessment of RC frame capacity subjected to a loss of corner column”, *Journal of Structural Engineering*, v. 148, n. 9, pp. 04022122, 2022. doi: [http://dx.doi.org/10.1061/\(ASCE\)ST.1943-541X.0003423](http://dx.doi.org/10.1061/(ASCE)ST.1943-541X.0003423).
- [16] ZHANG, W., KANG, S., LIN, B., *et al.*, “Mixed-mode debonding in CFRP-to-steel fiber-reinforced concrete joints”, *Journal of Composites for Construction*, v. 28, n. 1, pp. 04023069, 2024. doi: <http://dx.doi.org/10.1061/JCCOF2.CCENG-4337>.
- [17] ZHOU, C., WANG, J., SHAO, X., *et al.*, “The feasibility of using ultra-high performance concrete (UHPC) to strengthen RC beams in torsion”, *Journal of Materials Research and Technology*, v. 24, pp. 9961–9983, 2023. doi: <http://dx.doi.org/10.1016/j.jmrt.2023.05.185>.
- [18] YAO, X., LYU, X., SUN, J., *et al.*, “AI-based performance prediction for 3D-printed concrete considering anisotropy and steam curing condition”, *Construction & Building Materials*, v. 375, pp. 130898, 2023. doi: <http://dx.doi.org/10.1016/j.conbuildmat.2023.130898>.
- [19] DJONO, L., KAROLINA, R., *The effect of admixture Type F and silica fume on high early strength self-compacting concrete*, Indonesia, ACEIVE, 2018.
- [20] CARBALLOSA, P., GARCÍA CALVO, J.L., REVUELTA, D., *et al.*, “Influence of cement and expansive additive types in the performance of self-stressing and self-compacting concretes for structural elements”, *Construction & Building Materials*, v. 93, pp. 223–229, 2015. doi: <http://dx.doi.org/10.1016/j.conbuildmat.2015.05.113>.
- [21] VENKATESWARLU, K., DEO, S.V., MURMU, M., “Overview of effects of internal curing agents on low water to binder concretes”, *Materials Today: Proceedings*, v. 32, pp. 752–759, 2020. doi: <http://dx.doi.org/10.1016/j.matpr.2020.03.479>.
- [22] PAUL, A.M., GEORGE, E.H., “Self-compacting self-curing concrete: a review”, *International Research Journal of Engineering And Technology*, v. 5, n. 11, pp. 617–620, 2018.
- [23] KAMAL, M.M., SAFANA, M.A., BASHANDYA, A.A., *et al.*, “Experimental investigation on the behavior of normal strength and high strength self-curing self-compacting concrete”, *Journal of Building Engineering*, v. 16, pp. 79-93, 2018. doi: <http://dx.doi.org/10.1016/j.job.2017.12.012>.
- [24] AHMAD, S., AHMAD, M., “Effect of fly ash on the workability and mechanical properties of self-compacting concrete”, *Construction & Building Materials*, v. 133, pp. 223–229, 2017.
- [25] SENSALÉ, G.R., CAPPELLETTI, G., “Sustainability of self-compacting concrete with fly ash: from an eco-compatibility assessment to potential market penetration”, *Journal of Cleaner Production*, v. 201, pp. 294–309, 2018.
- [26] SONEBI, M., SUBHANI, M., “Rheological properties of self-compacting concrete containing fly ash”, *Cement and Concrete Composites*, v. 72, pp. 139–152, 2016.
- [27] LIU, S., WU, Z., WANG, D., *et al.*, “Effects of nano-silica and fly ash on the properties of self-compacting concrete”, *Construction & Building Materials*, v. 237, pp. 117588, 2020.

- [28] SRINIVAS PRABHU, R., ANURADHA, R., VIVEK, S., “Experimental research on triple blended self-concrete geo polymer concrete”, *Asian Journal of Engineering and Applied Technology*, v. 5, n. 2, pp. 15–21, 2016. <http://dx.doi.org/10.51983/ajeat-2016.5.2.804>.
- [29] NAVEEN ARASU, A., NATARAJAN, M., BALASUNDARAM, N., *et al.*, “Optimization of high performance concrete composites b using nano materials”, *Research on Engineering Structures and Materials*, 2023.
- [30] LIU, K., SHUI, Z., SUN, T., *et al.*, “Effects of combined expansive agents and supplementary cementitious materials on the mechanical properties, shrinkage and chloride penetration of self-compacting concrete”, *Construction & Building Materials*, v. 211, pp. 120–129, 2019. doi: <http://dx.doi.org/10.1016/j.conbuildmat.2019.03.143>.
- [31] SHEN, P., LU, L., HE, Y., *et al.*, “Investigation on expansion effect of the expansive agents in ultra-high performance concrete”, *Cement and Concrete Composites*, v. 105, pp. 103425, 2020. doi: <http://dx.doi.org/10.1016/j.cemconcomp.2019.103425>.
- [32] NAVEEN ARASU, N., NATARAJAN, M., BALASUNDARAM, N., *et al.*, “Utilizing recycled nanomaterials as a partial replacement for cement to create high performance concrete”, *Global NEST Journal*, v. 6, n. 25, pp. 89–92, 2023.
- [33] AKSHANA, V., NAVEEN ARASU, A., KARTHIGAISELVI, P., “Experimental study on concrete by partial replacement cement with silica fume”, *Journal of Critical Reviews*, v. 7, n. 17, pp. 3801–3805, 2020.
- [34] GANAPATHY, G.P., ALAGU, A., RAMACHANDRAN, S., *et al.*, “Effects of fly ash and silica fume on alkalinity, strength and planting characteristics of vegetation porous concrete”, *Journal of Materials Research and Technology*, v. 24, n. May-June, pp. 5347–5360, 2023. doi: <http://dx.doi.org/10.1016/j.jmrt.2023.04.029>.
- [35] NAVEEN ARASU, A., VIVEK, S., ROBINSON, J., *et al.*, “Experimental analysis of waste foundry sand in partial replacement of fine aggregate in concrete”, *International Journal of Chemtech Research*, v. 10, pp. 605–622, 2017.
- [36] WANG, Z., WANG, Q., JIA, C., *et al.*, “Thermal evolution of chemical structure and mechanism of oil sands bitumen”, *Energy*, v. 244, pp. 123190, 2022. doi: <http://dx.doi.org/10.1016/j.energy.2022.123190>.
- [37] YU, J., ZHU, Y., YAO, W., *et al.*, “Stress relaxation behaviour of marble under cyclic weak disturbance and confining pressures”, *Measurement*, v. 182, pp. 109777, 2021. doi: <http://dx.doi.org/10.1016/j.measurement.2021.109777>.
- [38] REN, C., YU, J., LIU, S., *et al.*, “A plastic strain-induced damage model of porous rock suitable for different stress paths”, *Rock Mechanics and Rock Engineering*, v. 55, n. 4, pp. 1887–1906, 2022. doi: <http://dx.doi.org/10.1007/s00603-022-02775-1>.
- [39] ZHANG, X., ZHOU, G., LIU, X., *et al.*, “Experimental and numerical analysis of seismic behaviour for recycled aggregate concrete filled circular steel tube frames”, *Computers and Concrete*, v. 31, n. 6, pp. 537–543, 2023. doi: <http://dx.doi.org/10.12989/cac.2023.31.6.537>.
- [40] ZHANG, X., LIU, X., ZHANG, S., *et al.*, “Analysis on displacement-based seismic design method of recycled aggregate concrete-filled square steel tube frame structures”, *Structural Concrete*, v. 24, n. 3, pp. 3461–3475, 2023. doi: <http://dx.doi.org/10.1002/suco.202200720>.